CROATICA CHEMICA ACTA
CCACAA **76** (1) 7–17 (2003)

ISSN-0011-1643
CCA-2847
Original Scientific Paper

Influence of Silica Sources on the Chemical Composition of Aluminosilicate Hydrogels and the Results of Their Hydrothermal Treatment

Ivan Krznarić,[a] Tatjana Antonić,[a] Josip Bronić,[a] Boris Subotić,[a,*] and Robert W. Thompson[b]

[a]*Laboratory for the Synthesis of New Materials, Ruđer Bošković Institute, Bijenička 54, 10000 Zagreb, Croatia*

[b]*Department of Chemical Engineering, Worcester Polytechnic Institute, 100 Institute Road, Worcester, MA 01609, USA*

RECEIVED NOVEMBER 29, 2001; REVISED MAY 15, 2002; ACCEPTED JULY 9, 2002

Among the parameters that influence the outcome of a hydrothermal synthesis of molecular sieve zeolites, the effects of various silica sources are some of the least understood. Prior studies have noted that some silica sources were »active,« or »inactive,« and there have been some suggestions that aluminium impurities can contribute to a silica source's »activity« to promote certain zeolite syntheses. However, a silica source's activity toward promoting zeolite crystallization has not been definitively shown to be linked to any specific impurity in the silica. This study reports on the use of four different silica sources and the corresponding distribution of Na, Al, and Si between the supernatant and amorphous gel phases. It is shown that the distribution of these species was unaffected by the choice of the silica source, but did vary with batch composition. Furthermore, the degree of silicate polycondensation (DPS), measured by the molybdate method, did not vary with the choice of the silica source. The observed differences in particulate and structural properties of the products crystallized from four different silica sources were analyzed in terms of the critical processes of zeolite crystallization (gel dissolution, nucleation, crystal growth).

Key words
aluminosilicate gels
precipitation
silica source
chemical composition
hydrothermal treatment
zeolite
crystal size

INTRODUCTION

It is well known that the course of crystallization and the structural, morphological and particulate properties of almost all known types of zeolites depend considerably on many factors, which may be collectively recognized as »synthesis conditions.« The influences of some of these factors are well known, and some of them have been intensely researched for decades, but others inspire researchers only periodically. One such parameter is the influence of the silica source on the course of crystallization and the structural, morphological, and particulate properties of crystallized zeolites resulting from the use of different silicas.

It is not known when, where, or by whom this effect was first noted, but Freund first openly reported on it in his article »Mechanism of the crystallization of zeolite X«, published in 1976 in the *Journal of Crystal Growth*.[1] Later, the existence of this effect was confirmed by the results of Lowe and coworkers.[2]

Freund[1] explained this effect by the presence of different amounts of Al^{3+} ions in different silica sources; *i.e.*, he suggested that the presence of Al^{3+} ions caused the

* Author to whom correspondence should be addressed. (E-mail: subotic@rudjer.irb.hr)

formation of hydroxylated anions of the $[HO–(SiO_3)_m–AlO_2–(SiO_3)_n–OH]^{(2m+2n+1)^-}$ type in »active« silicates. When the impure hydrated silicate was dissolved in water, these anion impurities as a whole had to go into solution and immediately act as nuclei of zeolites. Lowe and coworkers gave a similar explanation.[2]

Hamilton and coworkers[3] and Wiersema and Thompson[4] reported that the number of crystals of zeolite NaX and analcime, respectively, strongly depended on the silica source with everything else held constant. In the first report,[3] the concentrations of four impurities in the silica source were shown to correlate with the extent of nucleation, but no specific impurity could be uniquely identified to play a role in zeolite nucleation. In another study on the effects of varying the silica source[4] it was reported that analcime crystal growth rates in the four solutions were uniform, even though the nucleation behaviour was different. The yields of analcime from these experiments were different, however, and pointed to different nucleation rates in each system. These differences were suggested to stem from materials inherent in the silica sources, since the water, sodium hydroxide and alumina used in all of these systems were the same.

On the other hand, several research groups have reported observing nanometer-sized particulates in synthesis solutions both prior to the onset of crystallization and at the end of the process.[5–15] Shoeman[10] suggested that the nanometer-sized particulates could be the site of nucleation, based on the observation that they appeared to be the same size as the growing crystals, when extrapolated back to the beginning of the synthesis. He also noted their presence throughout the synthesis. Gora *et al.*[11] observed particulates in the silicate solution prior to mixing it with the aluminate solution, and noted that they persisted throughout the synthesis of zeolite NaA. No nanometer-sized particulates were found in the silicate solutions prepared in an unpublished study,[16] in which Hamilton's batch composition and four of his silica sources were used for the synthesis of zeolite NaX.[3] Hence, the origin of these particulates and the role they play in zeolite nucleation has been the subject of inquiry, but these questions have not been answered to date.

Finally, in many recent studies, the rate of dissolution/depolymerization and hydrolysis, respectively, of the silica source was identified as a critical factor that determines the pathway of crystallization and structural and particulate properties of crystallized zeolite(s).[17–28] Assuming that the rate of dissolution/depolymerization of the silica source influences the concentration of silica and distribution of different silicate and aluminosilicate species in the liquid phase of the crystallizing system,[17–21,26,27,29] the silica source may affect the type(s) of zeolite(s),[17–19,22] crystal size[19–21,23–28] and morphology,[23,24,28] and the rate of crystallization.[17,18,21–27] A recent study[29] focused on the same batch composition used by Hamilton, *et al.*[3] to synthesize zeolite NaX, and several of the same silica powders were utilized. An analysis of the degree of silica polycondensation (DPS) showed that the DPS in freshly prepared silicate solutions did not depend on the silica source.[29] On the other hand, DPS analysis of the silicate solutions prepared from different silica sources, but aged at room temperature for 44 days, indicated that the DPS increased with increasing content of water (of hydration) in the silica source.[17] The DPS in the silicate solution may influence the chemical composition of the amorphous aluminosilicate precipitated by mixing the silicate and aluminate solutions. Thus, it is possible that the silica source influences the course of crystallization and the properties of the crystalline end product(s) by altering the distribution of Na, Al, and Si between the solid and the liquid phases of the hydrogel.

In order to test this hypothesis, we report here on the analyses of the equilibrium distributions of Na_2O, Al_2O_3, and SiO_2 between the solid and liquid phases of the gels formed by mixing appropriate amounts of a common sodium aluminate solution with sodium silicate solutions prepared from different silica sources. Results of the analyses of the structural and particulate properties of the products obtained after the hydrothermal treatment of the gels prepared from different silica sources are also reported.

EXPERIMENTAL

Amorphous aluminosilicate gels having the batch compositions $x\ Na_2O \cdot Al_2O_3 \cdot y\ SiO_2 \cdot z\ H_2O$ were prepared by pipetting 50 ml of a sodium silicate solution with appropriate concentrations of Na_2O and SiO_2 into a plastic beaker containing 50 ml of a stirred sodium aluminate solution having appropriate concentrations of Na_2O and Al_2O_3. The compositions of the batches prepared for all syntheses are reported in Table I, and are identified as N = I–V. Sodium silicate solutions (approximately 0.8 M in SiO_2) having appropriate amounts of NaOH were prepared by: dilution of water-glass solution (Galenika; 9.64 % Na_2O, 28.07 % SiO_2) with sodium hydroxide solutions of appropriate concentrations (system I), dissolution of Na_2SiO_3 (Fluka AG; 51 % Na_2O, 48 % SiO_2) (system II) and $Na_2SiO_3 \cdot 5\ H_2O$ (Fluka AG; 28.4 % Na_2O, 27.5 % SiO_2) (system III) in sodium hydroxide solutions of appropriate concentrations, and dissolution of fumed silica (Aldrich; 99.8 % SiO_2) (system IV) and precipitated silica (Ventron; 99.5 % SiO_2) (system V) in hot sodium hydroxide solutions of appropriate concentrations. All percents used express mass fractions (100 w). The number of the system (I–V) corresponds to the silica source used.

Sodium aluminate solutions (0.1 to 0.32 M in Al_2O_3) were prepared by dissolving of anhydrous $NaAlO_2$ (54 % Al_2O_3 and 41% Na_2O) in sodium hydroxide solutions of appropriate concentrations. The solutions were thermostated at 25 °C, and the silicate solution was poured into the vigorously stirred aluminate solution in about 10 s. The formed hydrogel was stirred with a propeller for 10 min prior to

TABLE I. Source of silica (systems) and batch compositions of the starting sodium silicate and sodium aluminate solutions used for preparation of hydrogels

System-batch	Source of silica	Sodium silicate solution		Sodium aluminate solution[(a)]	
		$[Na_2O]$ / mol dm^{-3}	$[SiO_2]$ / mol dm^{-3}	$[Na_2O]$ / mol dm^{-3}	$[Al_2O_3]$ / mol dm^{-3}
I-1	Water-glass	1.507	0.823	0.418	0.335
I-2	Water-glass	1.517	0.853	0.130	0.104
II-1	Na_2SiO_3	1.576	0.784	0.403	0.323
II-2	Na_2SiO_3	1.579	0.819	0.130	0.104
III-1	$Na_2SiO_3 \cdot 5H2O$	1.565	0.839	0.414	0.332
III-2	$Na_2SiO_3 \cdot 5H2O$	1.571	0.841	0.130	0.104
IV-1	fumed silica	1.517	0.816	0.405	0.325
IV-2	fumed silica	1.519	0.835	0.128	0.102
V-1	precipitated silica	1.510	0.825	0.412	0.330
V-2	precipitated silica	1.541	0.837	0.132	0.106

[(a)]All sodium aluminate solutions were prepared by dissolution of anhydrous $NaAlO_2$ salt in NaOH solutions of appropriate concentrations.

further treatment. Batches b = 1 and 2 in systems I–V are distinguished by the values of $X = [Na_2O]_{bN} / [Al_2O_3]_{bN}$, $Y = [SiO_2]_{bN} / [Al_2O_3]_{bN}$, and $Z = [H_2O]_{bN} / [Al_2O_3]_{bN}$, where $[Na_2O]_{bN}$, $[Al_2O_3]_{bN}$, and $[SiO_2]_{bN}$ are the total amount concentrations of Na_2O, Al_2O_3, and SiO_2 in the formed hydrogels. The values of X ($X \approx 6$ for batch 1 and $X \approx 16$ for batch 2), Y ($Y \approx 2.5$ for batch 1 and $Y \approx 8$ for batch 2) and Z ($Z \approx 340$ for batch 1 and $Z \approx 1060$ for batch 2), determined by chemical analyses of batches b = 1 and 2 precipitated in systems N = I–V, are listed in Table II. The values of $[Na_2O]_{bN}$, $[Al_2O_3]_{bN}$ and $[SiO_2]_{bN}$ (in mol/dm^3) were calculated using the analytical data of the amounts of Na, Al and Si (in mg/kg) and the densities of the appropriate silicate and aluminate solutions.

TABLE II. Amount concentrations $[Al_2O_3]_{bN}$ and ratios $X = [Na_2O]_{bN} / [Al_2O_3]_{bN}$, $Y = [SiO_2]_{bN} / [Al_2O_3]_{bN}$ and $Z = [H_2O]_{bN} / [Al_2O_3]_{bN}$ in batches of systems I–V

System-batch	$[Al_2O_3]_{bN}$ / mol dm^{-3}	X	Y	Z
I-1	0.1673	5.754	2.460	331.77
I-2	0.0520	15.837	8.203	1068.57
II-1	0.1613	6.135	2.430	344.78
II-2	0.0521	16.323	7.864	1067.09
III-1	0.1658	5.969	2.530	334.98
III-2	0.0521	16.324	8.073	1067.33
IV-1	0.1623	5.921	2.510	343.16
IV-2	0.0512	16.085	8.156	1087.77
V-1	0.1650	5.824	2.500	337.37
V-2	0.0528	15.840	7.928	1053.74

Each of the prepared hydrogels was divided in two portions: one portion was put into plastic cuvettes of 50 ml and the other portion was put into PTFE vessels of 50 ml. The cuvettes containing the gels were tightly plugged with plastic stoppers and weighed. Both the cuvettes and the PTFE vessels with the hydrogels were sealed and kept in a water bath thermostated at 25 °C for 48 h.[30–32]

The hydrogels aged in the cuvettes were centrifuged to separate the solid from the liquid phase. After removal of the supernatant, the solid phase was redispersed in distilled water and centrifuged repeatedly. The procedure was repeated until the pH value of the liquid phase above the sediment was 9. The wet washed solids were dried overnight at 105 °C and cooled in a desiccator over silica gel. The dry solids were pulverized in an agate mortar. The pulverized solid samples were kept in a desiccator with saturated NaCl solution for 96 h. Thus prepared solids were used for powder X-ray diffractometry and differential thermal gravimetry. A part of each sample was calcined at 800 °C for 2 h. After cooling to ambient temperature in a desiccator over dry silicagel, a given amount of each of the calcined samples was dissolved in 1:1 HCl solution. The obtained solutions were diluted with distilled water to the concentration ranges suitable for measuring the concentrations of sodium, aluminium and silicon by atomic absorption spectroscopy.

The PTFE vessels with the hydrogels aged at 25 °C for 48 hours were sealed in stainless-steel reaction vessels, and put into an oven preheated to the crystallization temperature (80 °C). In preliminary experiments, small volumes of the reaction mixture were drawn off the system and observed using a light microscope. The time at which no amorphous phase was observed was used as the end of the crystallization process. Completion of the crystallization process was also revealed by the powder X-ray diffraction analysis of the

crystalline end products. Hence, the hydrogels were heated under static conditions at 80 °C for predetermined reaction times, *i.e.*, until the amorphous aluminosilicate was completely transformed to crystalline phase(s). Following cooling, the crystalline products were separated from the liquid phase by centrifugation, washed with distilled water and dried overnight at 105 °C. The dry crystalline solids were used for powder X-ray diffraction, scanning-electron microscopy, and determination of the particle-size distribution.

Concentrations of sodium, aluminum, and silicon in the solutions obtained by the dilution of the supernatants and dissolving the calcined samples were measured by a Perkin-Elmer 3030B Atomic Absorption Spectrometer. The measured concentrations of Na, Al, and Si were used to determine of the equilibrium chemical compositions of the solid (precipitated aluminosilicate) and liquid (supernatants) phases of hydrogels.

The degree of Si polycondensation in the starting sodium silicate solutions and in the supernatants (after solid-liquid separation) was determined by the molybdate method.[33] The method is based on the reaction of monosilicic acid with the molybdic acid, and thus the formation of a yellow-colored complex. The kinetics of the reaction depends on the amount fraction of monomeric silicate anions in a mixture with other silicate species (dimers, trimers, *etc.*) and may be expressed as a function of the logarithm of the fraction (100 x) of unreacted SiO_2, ln *UR*, against the reaction time, t_R. To determine the fractions of monomeric and dimeric silicate anions in the supernatants, the experimentally determined ln *UR vs.* t_R plots were compared with the ln *UR vs.* t_R functions calculated by the relation:

$$UR = D_0 \exp(-k_2\, t_R) + \exp(-k_3\, t_R)\{M_0 + [k_2 D_0/(k_3 - k_2)]\,[\exp(k_3 - k_2)\, t_R - 1]\} \quad (1)$$

derived[34] on the basis of O'Connor's study,[35] where M_0 and D_0 are the amount fractions (x/%) of monomers and dimers in the reaction mixture at the time $t_R = 0$, k_2 (= 0.9 min^{-1}) is the rate constant of the dimer hydrolysis to monomers[33] and k_3 (= 1.7 min^{-1}) is the rate constant of the reaction of monosilicic acid with the molybdic acid for the formation of the colored complex.[35]

The X-ray powder diffraction patterns of samples (washed precipitated solids and the solid phases obtained by the hydrothermal treatment of the hydrogels) were collected using a Philips PW 1820 Vertical goniometer mounted on a Philips PW 1300 X-ray generator (Cu-Kα radiation) in the region of Bragg angles 2θ = 10–46°. The relative amounts of crystalline phases (zeolites A, X and P) present in the crystalline end products were determined using an external standard method.[36]

SEM photomicrographs of the crystalline end products obtained by the hydrothermal treatment of the hydrogels were made with a SEM 515 (Philips) scanning electron microscope.

Particle size distribution curves of the solid samples were determined with a Malvern Mastersize XLB laser light-scattering particle-size analyzer.

RESULTS AND DISCUSSION

Figure 1 shows the kinetics of the reactions of silicate anions with molybdic acid from the starting silicate solutions prepared from different silica sources, denoted as systems I–V in Table I. The kinetics, expressed as a function of the already explained (in Experimental), ln *UR versus* t_R did not depend on the silica source used. Since the rate of the reaction of silicate anions with molybdic acid depends on the degree of polycondensation of the silicate anions (DPS),[33,35,37,38] the independence of the reaction rate of the source of silica in Figure 1 indicated that the DPS of the silicate anions in the solutions did not depend on the silica source, but on the concentrations of SiO_2 and Na_2O in the solutions. An analysis of the ln *UR versus* t_R curves showed that the starting silicate solutions contained only monomeric and dimeric silicate anions. By comparing the measured reaction kinetics (data symbols) with the calculated ones (solid curves) in Figure 1, it may be estimated that all solutions initially contained the same fractions of monomers (*ca.* 65 %) and dimers (*ca.* 35 %).

Addition of a silicate solution to an aluminate solution results in instantaneous precipitation of an amorphous aluminosilicate gel. Concentrations of Na, Al, and Si (in mg/kg) in the supernatants were determined after ageing and solid-liquid separation. We also determined the densities of all starting aluminate and silicate solutions as well as the liquid phases (supernatants) after centrifugation. Furthermore, we quantitatively determined the amount of the precipitated solid phase. Using these data, the con-

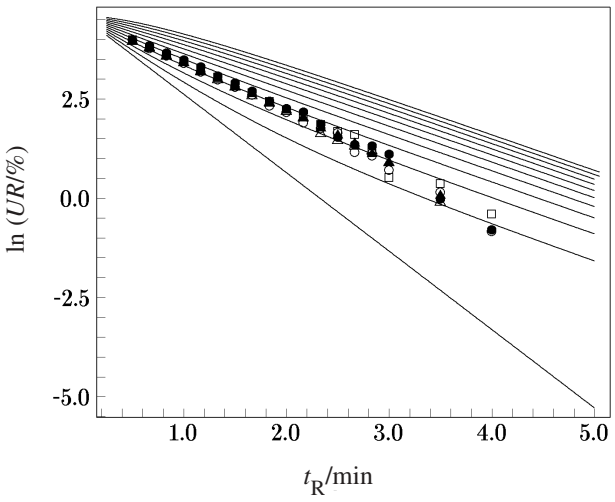

Figure 1. Logarithm of the amount fraction of SiO_2 unreacted with molybdic acid, ln *UR*, plotted as a function of the reaction time, t_R, of the molybdic acid with silicate anions in the starting silicate solutions prepared with water glass (○; system I), Na_2SiO_3 (●; system II), $Na_2SiO_3 \cdot 5H_2O$ (△; system III), fumed silica (▲; system IV) and precipitated silica (□; system IV). The solid curves (from the bottom to the top) correspond to the reaction of monomers and dimers in the solutions containing 0, 10, 20, 80, 90 and 100 % of dimers with molybdic acid, calculated by Eq. (1).

TABLE III. Concentrations of Na_2O, Al_2O_3 and SiO_2 distributed between the liquid (L) and the solid (S) phases in batches $b = 1$ and 2 of systems N = I–V

System-batch	$[Al_2O_3]_{bN}$ / mol dm^{-3}	$[Na_2O]_L$ / mol dm^{-3}	$[Na_2O]_S$ / mol dm^{-3}	$[Al_2O_3]_L$ / mol dm^{-3}	$[Al_2O_3]_S$ / mol dm^{-3}	$[SiO_2]_L$ / mol dm^{-3}	$[SiO_2]_S$ / mol dm^{-3}
I-1	0.1673	0.8260	0.1367	0.0301	0.1372	0.0645	0.3471
I-2	0.0520	0.7673	0.0562	0.0009	0.0511	0.2568	0.1698
II-1	0.1613	0.8553	0.1344	0.0321	0.1292	0.0642	0.3278
II-2	0.0521	0.8015	0.0490	0.0031	0.0489	0.2422	0.1675
III-1	0.1658	0.8540	0.1356	0.0274	0.1384	0.0652	0.3543
III-2	0.0521	0.7985	0.0520	0.0007	0.0513	0.2481	0.1726
IV-1	0.1623	0.8300	0.1311	0.0301	0.1322	0.0655	0.3425
IV-2	0.0512	0.7726	0.0509	0.0007	0.0505	0.2463	0.1712
V-1	0.1659	0.8277	0.1333	0.0331	0.1328	0.0645	0.3478
V-2	0.0528	0.7861	0.0503	0.0036	0.0492	0.2470	0.1716

centrations $[Na_2O]_L$, $[Al_2O_3]_L$, and $[SiO_2]_L$ (the amounts of Na_2O, Al_2O_3 and SiO_2 in the liqud phases contained in 1 dm^3 of hydrogel) were calculated. Then, using these values, as well as the data on the amounts of Na, Al, and Si in the whole system ($[Na_2O]_{bN}$, $[Al_2O_3]_{bN}$ and $[SiO_2]_{bN}$), the values of $[Na_2O]_S$, $[Al_2O_3]_S$, and $[SiO_2]_S$ in the precipitated amorphous aluminosilicate samples (the amounts of Na_2O, Al_2O_3 and SiO_2 in the precipitate contained in 1 dm^3 of hydrogel) were calculated as:

$$[Me_aO_b]_S = [Me_aO_b]_{bN} - [Me_aO_b]_L \quad (2)$$

where $Me_aO_b = Na_2O$, Al_2O_3 and/or SiO_2, and $[Me_aO_b]_{bN}$ represents the batch concentrations of Na_2O, Al_2O_3 and/or SiO_2 (in mol/dm$_3$). The corresponding values of $[Me_aO_b]_S$ and $[Me_aO_b]_L$ are listed in Table III.

Mole ratios, $X_S = [Na_2O]_S / [Al_2O_3]_S$ and $Y_S = [SiO_2]_S / [Al_2O_3]_S$ in the solid phases reported in Table IV, were determined in two different ways:[30–32]

(i) Using the data of the chemical analysis (Na, Al, Si) in the solid phase. Since these ratios were determined by a direct analysis of the solid phase, they are denoted as $X_S(S)$ and $Y_S(S)$, respectively.

(ii) Using the values of $[Me_aO_b]_S$ calculated by Eq. (2), *e.g.*,

$$X_S(L) = ([Na_2O]_{bN} - [Na_2O]_L) / ([Al_2O_3]_{bN} - [Al_2O_3]_L) \quad (3)$$

$$Y_S(L) = ([SiO_2]_{bN} - [SiO_2]L) / ([Al_2O_3]_{bN} - [Al_2O_3]_L) \quad (4)$$

The corresponding values of $X_S(S)$, $X_S(L)$, $Y_S(S)$ and $Y_S(L)$ are listed in Table IV.

The results of the chemical analyses of both the liquid and the solid phases of the aged hydrogels, presented in Tables III and IV, showed that:

(i) The values of $[Me_aO_b]_L$ and $[Me_aO_b]_S$, and, thus, the distribution of Na, Al, and Si between the solid and the liquid phases, depends on the chemical compositions of the silicate and aluminate solutions (Table I), and thus on the batch chemical composition of the systems (Table II).

(ii) The distribution of Na, Al, and Si between the solid and the liquid phases in the systems having a constant batch composition determined by the values of $[Al_2O_3]_{bN}$, X, Y, and Z do not depend on the silica source used for the preparation of the silicate solutions.

The increase of the values of $[SiO_2]_L$ and $[SiO_2]_S / [Al_2O_3]_S$ and the simultaneous decrease of the values of $[Al_2O_3]_L$, $[SiO_2]_S$ and $[Al_2O_3]_S$ with increasing value of $Y = [SiO_2]_{bN} / [Al_2O_3]_{bN}$ are in accord with the results of our previous studies,[31,32] and may be explained easily. First, all monomeric $Al(OH)_4^-$ anions from the aluminate

TABLE IV. Mole ratios $X_S(S)$ and $X_S(L)$ (= $[Na_2O]_S / [Al_2O_3]_S$), $Y_S(S)$ and $Y_S(L)$ (= $[SiO_2]_S / [Al_2O_3]_S$) in the solid samples precipitated in batches $b = 1$ and 2 of the systems N = I–V.

System-batch	$[Al_2O_3]_{bN}$ / mol dm^{-3}	$X_S(S)$	$X_S(L)$	$Y_S(S)$	$Y_S(L)$
I-1	0.1670	1.029	0.996	2.530	2.530
I-2	0.0520	1.123	1.099	3.323	3.322
II-1	0.1613	1.111	1.040	2.537	2.540
II-2	0.0521	1.092	1.002	3.425	3.419
III-1	0.1658	1.013	0.980	2.560	2.620
III-2	0.0521	1.133	1.014	3.365	3.356
IV-1	0.1623	1.096	0.992	2.591	2.586
IV-2	0.0512	1.260	1.008	3.390	3.392
V-1	0.1659	1.181	1.004	2.619	2.620
V-2	0.0528	1.182	1.022	3.488	3.562

[a] Symbols $X_S(S)$, $X_S(L)$, $Y_S(S)$ and $Y_S(L)$ are explained in the text.

solution[39] will react with silicate anions having different degrees of polycondensation[40–44] during the formation of the aluminosilicate gel skeleton.[45] Second, in solutions containing a mixture of silicate anions, aluminium preferentially complexes with the larger silicate species, and almost immediately.[46] Finally, the solubility of the precipitated amorphous aluminosilicate increases with the increase of both the total alkalinity, $[Na_2O]_{bN}$ and the ratio $[SiO_2]_S / [Al_2O_3]_S$.[31,32]

On the other hand, the values of $[Me_aO_b]_L$ and $[Me_aO_b]_S$ were not influenced by the silica source used for the preparation of silicate solutions, and they were constant for constant batch mole ratio Y $[SiO_2]_{bN} / [Al_2O_3]_{bN}$ (see Tables II and III). Hence, a constancy of the ratio $[SiO_2]_S / [Al_2O_3]_S \approx 2.5$ for $Y \approx 2.5$ ($b = 1$; see Table IV) and $[SiO_2]_S / [Al_2O_3]_S \approx 3.4$ for $Y \approx 8$ ($b = 2$; see Table IV) was observed. Additionally, Table V shows the constancy of the mass, m_S, of the dehydrated amorphous aluminosilicate precipitated (in 1 dm^3 of the batch) from the systems having constant batch compositions, *i.e.*, $m_S \approx 41.5$ g/dm^3 for $Y \approx 2.5$ and $m_S \approx 18.5$ g/dm^3 for $Y \approx 8$, as expected. While the ratios $Y_S = [SiO_2]_S / [Al_2O_3]_S$ determined in two different ways were almost the same, ratios $X_S(S) > 1$ were (considerably) higher than ratios $X_S(L) \approx 1$ (see Table IV). The value $X_S(S) > 1$ is probably caused by the residual (unwashed) Na_2O in the solid samples. On the other hand, the value $X_S(L) \approx 1$ is in agreement with the results of our previous analyses,[30–32] and indicates that Al in the gel skeleton is coordinated four-fold within the common (Si,Al,O) framework, whereas the Na^+ ions compensate for the excess negative charge of aluminium-oxygen tetrahedral.[45]

The value of m_S(calc.), calculated by the expression:

$$m_S = M_{Na_2O}[Na_2O]_S + M_{Al_2O_3}[Al_2O_3]_S + M_{SiO_2}[SiO_2]_S \quad (5)$$

TABLE V. Measured (meas.) and calculated (calc.) mass, m_S, of the dehydrated amorphous aluminosilicates (daa) precipitated in 1 dm^3 of batches 1 and 2 of systems I–V

System-batch	$[Al_2O_3]_{bN}$	m_S(daa) / g	
	mol dm^{-3}	meas.	calc.
I-1	0.1670	42.09	43.32
I-2	0.0520	13.50	18.90
II-1	0.1613	39.88	41.20
II-2	0.0521	12.73	18.08
III-1	0.1658	41.78	43.80
III-2	0.0521	13.74	18.82
IV-1	0.1623	40.06	42.18
IV-2	0.0512	14.22	18.59
V-1	0.1659	41.45	42.70
V-2	0.0528	12.76	18.45

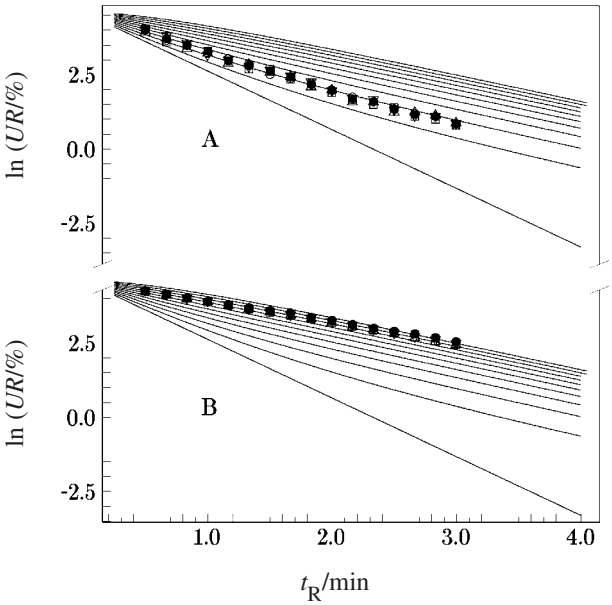

Figure 2. Logarithm of the fraction of SiO_2 unreacted with molybdic acid, ln *UR*, plotted as a function of the reaction time, t_R, of the molybdic acid with silicate anions in the liquid phases of batches 1 (A) and 2 (B) of systems I (○), II (△), III (▽), IV (□), and V (●). Solid curves (from the bottom to the top) correspond to the reaction of monomers and dimers in the solutions containing 0, 10, 20 … 80, 90 and 100 % of dimers with molybdic acid, calculated by Eq. (1).

(where, M_{Na_2O}, $M_{Al_2O_3}$ and M_{SiO_2} are the molecular weights and $[Na_2O]_S$, $[Al_2O_3]_S$ and $[SiO_2]_S$ are the concentrations of Na_2O, Al_2O_3 and SiO_2 contained in the solid phase precipitated in 1 dm^3 of the batch (see Table III)) are in very good agreement with the measured values, m_S(meas.) for batches 1 (see Table V). However, the calculated values of m_S in batches 2 are by *ca.* 40 % lower than the measured values (see Table V). The difference may be caused by the very low values of $[Al_2O_3]_L$ (see Table III) used for the calculation of the values of $[Al_2O_3]_S$ (in Eq. 3), and by the loss of the solid phase precipitated in batches 2 during washing.

Figure 2 shows the kinetics of the reactions of silicate anions with molybdic acid from the supernatant mother liquors of batches 1 (A) and 2 (B) of systems I (○), II (△), III (▽), IV (□) and V (●). The reaction rates were considerably higher in the liquid phases of batches 1 than batches 2, but they were almost the same for a given batch. Since the liquid phase concentration of $[SiO_2]_L$ and $[Na_2O]_L$ did not depend on the silica source at a constant mole ratio $Y = [SiO_2]_{bN} / [Al_2O_3]_{bN}$ (see Table III), the results presented in Figure 2 indicate that the DPS in the silicate solutions did not depend on the silica source either, but on the concentrations of SiO_2 and Na_2O in the solutions. Batches 1 had a lower DPS of silicate anions, with 70–80 % of monomers and 20–30 % of dimers compared to batches 2 which had mostly dimers. Consequently, higher reaction rates of silicate anions

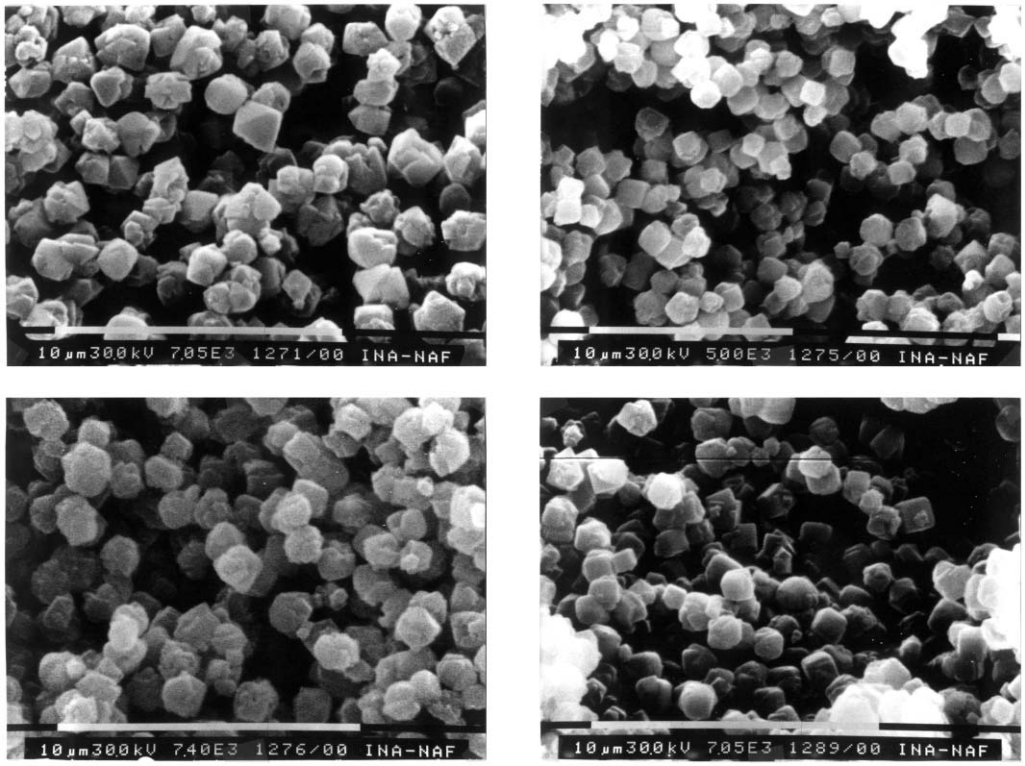

Figure 3. Scanning electron micrographs of the products of hydrothermal treatment (see Table VI) of batches 1 of systems (hydrogels) I (top-left), II (top-right), III (bottom-left), and IV (bottom-right).

with molybdic acid were observed in batches 1 compared to batches 2. This was expected,[19] due to the considerably lower $X_L = [Na_2O]_L / [SiO_2]_L$ in batches 1 ($X_L = 0.077$) than in batches 2 ($X_L = 0.32$).

While the chemical compositions of the solid and liquid phases of the hydrogels and the DPS of the silicate anions in the liquid phases were independent of the silica source, the particulate (batches 1 and 2) and structural properties (batches 1) of zeolites obtained by the hydrothermal treatment of the hydrogels depended considerably on the silica source. For example, the hydrothermal treatment of batches 2 ($Y \approx 8$) resulted in crystallization of the essentially pure zeolite X with only traces of zeolite P (see Table VI). Crystals of zeolite X formed in all systems (I-2 to IV-2) had the typical bipyramidal morphology (see Figure 4). On the other hand, the specific number (Table VI) and crystal size distribution of zeolite X crystals (see Figure 5B) depended on the silica source. Since the chemical compositions of both the solid and liquid phases were almost the same for a given batch in different systems (*e.g.* I-2 to IV-2; see Table III), it can be assumed that the rate of gel dissolution during heating did not depend on the silica source. Hence, it can be concluded that the growth rates of zeolite X crystals was the same in all systems (I-2 to IV-2),[3,4] and thus that the differences in the crystal size distributions of different products were caused by the variation in the number of nuclei formed in different systems rather than by the differences in the growth rates.[3,4] In accord with abundant evidence, due to the high supersaturation of constituents (Na, Si, Al, template) in gel,[11,47–49] most nuclei are formed in the gel and/or at the gel/liquid interface by linking of specific subunits during gel precipitation and/or ageing.[11,34,45,47,50–58] The number of nuclei formed in the gel matrix during its formation and ageing may be a function of the amount and structure of the hydroxylated anions present in the silicate solutions prepared with different silica sources.[1,2]

The same mechanism of nucleation may be assumed for batches 1. The number of nuclei formed in the gel matrix depends strongly on the silica source used for gel precipitation and increases in the sequence: system-I (water-glass) < system-II (Na_2SiO_3) < system-III ($Na_2SiO_3 \cdot 5H_2O$) < system-IV (fumed silica) (see Table VI). More nuclei, producing consequently smaller average crystal sizes (see Table VI) and narrower crystal size distributions of zeolite(s), crystallized in batches 2 than in batches 1 (see Figure 5), in accord with the results of the recent studies on the influence of the batch mole ratio Y on the particle size distribution of zeolites A[59,60] and X.[60] Heating of hydrogels causes dissolution of the gel matrix, releasing nuclei from the dissolved part of the gel.[34,45,51,60–62] The released nuclei start to grow from the supersaturated solution.[61–64] However, in contrast to the formation of nuclei with the faujasite structure, and thus preferential growth of zeolite X at the high

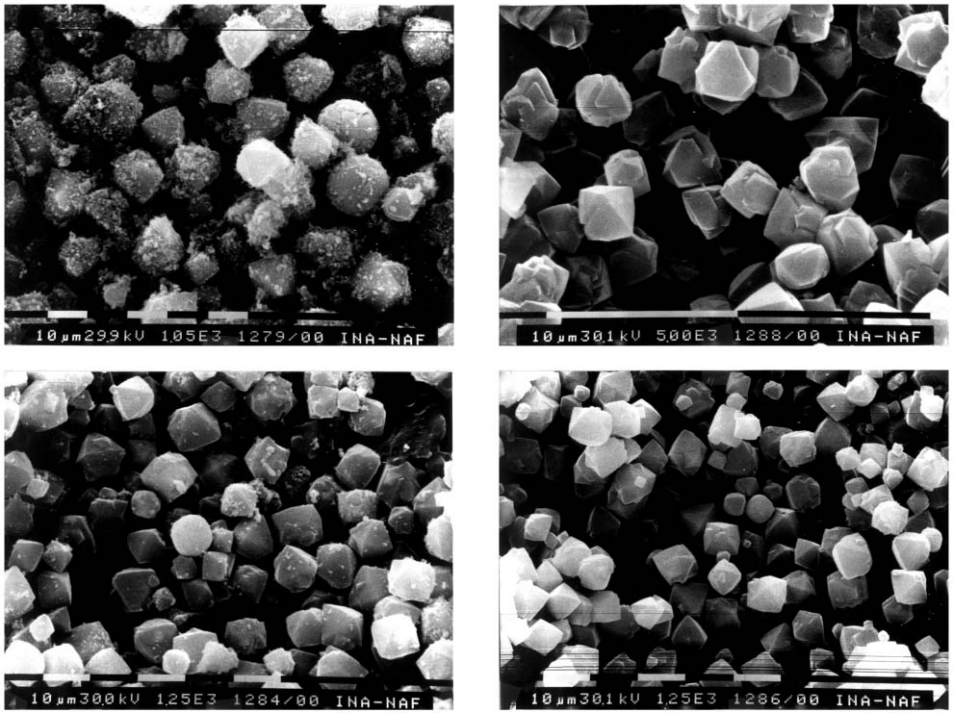

Figure 4. Scanning electron micrographs of the products of hydrothermal treatment (see Table VI) of batches 2 of systems (hydrogels) I (top-left), II (top-right), III (bottom-left), and IV (bottom-right).

batch mole ratio $Y = [SiO_2]_{bN} / [Al_2O_3]_{bN} \approx 8$, and correspondingly high $Y_L = [SiO_2]_L / [Al_2O_3]_L \approx 180$ (batches 2, see Table III), both 4-4 (building blocks of zeolite A nuclei) and 6-6 secondary building units (building blocks of faujasite nuclei) form in the gel matrix[52,65] at lower batch mole ratios, *e.g.*, $Y \approx 2.5$ (batches 1). Hence, both zeolites A and X may co-crystallize in the liquid phase of batches 1 ($Y_L \approx 2.2$; see Table III). This is in accord with the results of previously published studies of the influence of Y[66,67] and Y_L,[62,64] respectively, on the co-crystallization[62,64,66–68] of zeolites A and X. Taking into consideration that (i) both zeolites A[69] and X[70] may be spontaneously transformed into zeolite P, and (ii) the overall crystallization rate increases with increasing number of growing nuclei (crystals), it is evident that the amount of zeolite P, in the products obtained by hydrothermal treatment of batches 1 is a function of the duration of the crystallization process and the number of nuclei formed in the gel matrix. Hence, the amount of P increases with the decreasing number of nuclei, and thus with an increase of the time, t_{end}, needed for complete transformation of the amorphous aluminosilicate precursor into crystalline products (zeolites) (see Table VI). Hence, the number and type of nuclei formed in the gel matrix during its formation and ageing is a function of the amount and structure of the hydroxylated anions present in the silicate solutions prepared with different silica sources.[1,2]

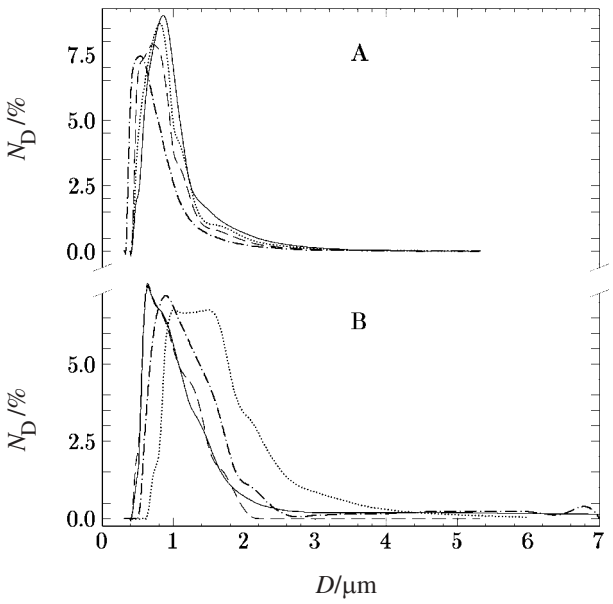

Figure 5. Particle size distribution curves of the products of hydrothermal treatment (see Table VI) of batches 1 (A) and 2 (B) of systems (hydrogels) I (solid curves), II (dotted curves), III (dashed curves), and IV (dot-dashed curves).

On the other hand, the variation of zeolites A and X in crystallization products (see Table VI) probably depends on (i) the proportion of nuclei of zeolite A and zeolite X as well as on the total number of nuclei formed in the gels prepared from different silica sources, (ii) the tendency of spontaneous transformation of 4-4 into 6-6 secondary building units (*e.g.*, an increase of the fraction

TABLE VI. Phase composition, average size $\overline{L}$, and specific number $\overline{N}$ of the products obtained by hydrothermal treatment (heating at 80 °C for an appropriate time, t_{end}) of batches 1 and 2 of systems (hydrogels) I–IV

System-batch	t_{end} / min	Phase composition[a]	$\overline{L}$ / mm	$\overline{N}$ / # g^{-1}
I-1	240	18 % A + 69 % X + 13 % P	0.93	3.64×10^{11}
I-2	440	X + traces P	1.12	8.05×10^{10}
II-1	180	65 % A + 27 % X + 8 % P	0.86	4.42×10^{11}
II-2	620	X + traces P	1.49	3.10×10^{10}
III-1	160	36 % A + 62 % X + 2 % P	0.80	5.48×10^{11}
III-2	430	X + traces P	0.99	9.32×10^{10}
IV-1	110	79 % A + 19 % X + 2 % P	0.68	8.39×10^{11}
IV-2	470	X + traces P	1.20	7.10×10^{10}

[a] A, zeolite A; X, zeolite X; P, zeolite P; #, number of nuclei and/or crystals.

of zeolite X nuclei and a simultaneous decrease of the fraction of zeolite A nuclei) during gel ageing,[52,65] and (iii) the difference in the growth rates of zeolites A and X.[64] However, since all the mentioned processes are interdependent and take place simultaneously, we expect that the observed effect will be better explained by the interpretation of the planned kinetic analyses.

CONCLUSIONS

Analyses of the distribution of Na_2O, Al_2O_3, and SiO_2 between the solid and liquid phases of the aluminosilicate hydrogels prepared at two different batch mole ratios, $Y = [SiO_2]_{bN} / [Al_2O_3]_{bN} = 2.5$ and 8, using five different silica sources (water-glass, Na_2SiO_3, $Na_2SiO_3 \cdot 5H_2O$, fumed silica, and precipitated silica) were carried out. The results from these studies, using various silicate solutions, have shown that:

– The kinetics of the reactions of silicate anions with molybdic acid from the starting silicate solutions prepared from different silica sources did not depend on the silica source used, but on the concentrations of SiO_2 and Na_2O in the solutions. It may be estimated that all solutions initially contained the same fractions of monomers (*ca.* 65 %) and dimers (*ca.* 35 %).

– The distribution of Na, Al, and Si between the solid and liquid phases depends on the chemical compositions of the silicate and aluminate solutions, and thus on the batch chemical composition of the systems, but not on the silica source used for the preparation of silicate solutions.

– The kinetics of the reactions of silicate anions with molybdic acid from the liquid phases of the hydrogels did not depend on the silica source used, but on the concentrations of SiO_2 and Na_2O in the solutions. A lower DPS of silicate anions in batches 1 (70–80 % of monomers and 20–30 % of dimers) than in batches 2 (mostly dimers) was caused by the considerably lower ratio $X_L = [Na_2O]_L / [SiO_2]_L$ in batches 1 ($X_L \approx 0.077$) than in batches 2 ($X_L \approx 0.32$).

– Hydrothermal treatment of batches 2 ($Y \approx 8$) resulted in formation of almost pure zeolite X (traces of zeolite P were present in all products). In contrast to the insensitivity of the distribution of Na, Al, and Si between the solid and liquid phases of the hydrogels and the type of zeolite crystallized (zeolite X) from the hydrogels on the silica source used, particulate properties of the products depended on the silica source. This indicated that the number of nuclei formed in the gel matrix during its formation and ageing may be a function of the amount and »structure« of the hydroxylated anions present in the silicate solutions prepared by different silica sources.

– Hydrothermal treatment of batches 1 ($Y \approx 2.5$) resulted in formation of different mixtures of zeolites A, X, and P. The number of nuclei formed in the gel matrix, and thus the specific number, $\overline{N}$, of crystals in the crystalline end product increases in the sequence: (water-glass) < (Na_2SiO_3) < ($Na_2SiO_3 \cdot 5H_2O$) < (fumed silica). Consequently, the time, t_{end}, needed for complete transformation of the amorphous aluminosilicate precursor into crystalline products (zeolites) increased with the decreasing number of nuclei, *i.e.* t_{end} (fumed silica) < t_{end} ($Na_2SiO_3 \cdot 5H2O$) < t_{end} (Na_2SiO_3) < t_{end} (water-glass). Hence, the observed decrease of the amount of zeolite P with increasing the number of nuclei may be explained by the tendency to transformation of metastable to more stable types of zeolites (A and X to P). Variation of zeolites A and X fractions in crystallization products is a complex function of the ratio of zeolite A and zeolite X nuclei formed in the gels prepared from different silica sources and the difference in the growth rates of zeolites A and X. However, since all the mentioned processes are interdependent and take place simultaneously, we expect that the observed effect will be better explained by interpretation of the planned kinetic analyses.

– Although the role of hydroxylated anions present in silicate solutions seems to be a reasonable explanation for the influence of silica source on the pathway of crystallization and the properties of crystallization products,

very different results obtained in separate studies indicate that the mode of gel preparation and treatment (especially ageing) as well as the crystallization conditions must be also considered in the interpretation of the results. Hence, a more complex investigation should be carried out to get a more complete understanding of the influence of silica source on the results of crystallization.

Acknowledgments. – This work was supported by the Ministry of Science and Technology of the Republic Croatia and by the National Science Foundation (NSF) through mediation of the U.S.-Croatian Joint Board of Scientific and Technological Cooperation.

REFERENCES

1. E. F. Freund, *J. Cryst. Growth* **34** (1976) 11–23.
2. B. M. Lowe, N. A. MacGilp, and T. V. Whittam, in: L. V. C. Rees (Ed.), *Proceedings of the 5th International Zeolite Conference* (Naples, Italy), Heyden, London-Philadelphia-Rheine, 1980, pp. 85–93.
3. K. E. Hamilton, E. N. Coker, A. Sacco, Jr., A. G. Dixon, and R. W. Thompson, *Zeolites* **13** (1993) 645–653.
4. G. S. Wiersema and R. W. Thompson, *J. Mater. Chem*. **6** (1996) 1693–1699.
5. O. Regev, Y. Cohen, E. Kehalt, and Y. J. Talmon, *Journal de Physique IV* **3** (1993) 397–400.
6. T. M. A. Twoomey, M. Mackay, H. P. C. E. Kuipers, and R. W. Thompson, *Zeolites* **14** (1994) 162–168.
7. O. Regev, Y. Cohen, E. Kehalt, and Y. J. Talmon, *Zeolites* **14** (1994) 314–319.
8. W. H. Dokter, T. P. M. Beelen, H. F. van Garderen, C. P. J. Rummens, R. A. van Santen, and J. D. F. Ramsay, *Coll. & Surf. A: Physchem & Eng. Asp*. **85** (1994) 89–95.
9. P. P. De Moor, T. P. M. Beelen, and R. A. van Santen, *Microporous Mater.* **9** (1997) 117–130.
10. B. J. Schoeman, *Zeolites* **18** (1997) 97–105.
11. L. Gora, K. Streletzky, R. W. Thompson, and G. D. J. Philies, *Zeolites* **18** (1997) 119–131.
12. C. E. A. Kirschhock, R. Ravishankar, F. Verspeurt, P. J. Grobet, P. A. Jacobs, and J. A. Martens, *J. Phys. Chem*. **103** (1999) 4956–4971.
13. C. E. A. Kirschhock, R. Ravishankar, L. Van Looveven, P. A. Jacobs, and J. A. Martens, *J. Phys. Chem.* **103** (1999) 4972–4978.
14. C. E. A. Kirschhock, R. Ravishankar, P. A. Jacobs, and J. A. Martens, *J. Phys. Chem*. **103** (1999) 11021–11027.
15. V. Nikolakis, E. Kokkoli, M. Tirrell, M. Tsapatsis, and D. G. Vlachos, *Chem. Mater.* **12** (2000) 845–853.
16. R. W. Thompson and T. Antonić, results of an unpublished study, WPI, 1998.
17. F.-Y. Dai, M. Suzuki, H. Takahashi, and Y. Saito, in: M. L. Occelli and H. E. Robson (Eds.), *Zeolite Synthesis*, *ACS Symp. Ser. No. 398,* Am. Chem. Soc., 1989, pp. 244–256.
18. R. Hino and Y. Moriya, *Mem. Fac. Sci. Shimane Univ.* **28** (1994) 47–58.
19. J. Warzywoda, A. G. Dixon, R. W. Thompson, A. Sacco, Jr., and S. L. Suib, *Zeolites* **16** (1996) 125–137.
20. J. Warzywoda, A. G. Dixon, R. W. Thompson, A. Sacco, Jr., *J. Mater. Chem.* **5** (1995) 1019–1025.
21. G. Zhu, S. Qiu, J. Yu, F. Gao, F. Xiao, R. Xu, Y. Sakamoto, and O. Terasaki, in: M. M. J. Treacy, B. K. Marcus, M. E. Bisher, and J. B. Higgins (Eds.), *Proceedings of the 12th International Zeolite Conference*, (Baltimore, MD.), Material Research Society, Warrendale, PA, 1999, pp. 1863–1870.
22. T. Kubota, Y. Oumi, T. Uozumi, and T. Sano, *Nippon Kagaku Kaishi,* (October 2000) 733–737.
23. H. Kalipcilar and A. Culfaz, *Cryst. Res. Technol.* **35** (2000) 933–942.
24. H. Kalipcilar and A. Culfaz, *Cryst. Res. Technol*. **36** (2001) 1197–1207.
25. Q. H. Li, B. Mihailova, D. Creaser, and J. Sterte, *Microporous Mesoporous Mater.* **43** (2001) 51–59.
26. Y. S. Ko, S. H. Chang, and W. S. Ahn, in: A. Galarneau, F. Di Renzo, F. Fajula, and J. Vedrine (Eds.), *Zeolites and Mesomorphous Materials, Studies of Surface Science and Catalysis,* Vol. 135, Elsevier, Amsterdam, 2001, p. 02-P-19.
27. W. Schmidt, A. Toktarev, F. Schüth, K. G. Ione, and K. Unger, in: A. Galarneau, F. Di Renzo, F. Fajula, and J. Vedrine (Eds.), *Zeolites and Mesomorphous Materials, Studies of Surface Science and Catalysis,* Vol. 135, Elsevier, Amsterdam, 2001, p. 02-P-23.
28. F. Hamidi, M. Pamba, A. Bengueddach, F. Di Renzo, and F. Fajula, in: A. Galarneau, F. Di Renzo, F. Fajula, and J. Vedrine (Eds.), *Zeolites and Mesomorphous Materials, Studies of Surface Science and Catalysis,* Vol. 135, Elsevier, Amsterdam, 2001, p. 02-P-29
29. T. Antonić, B. Subotić, V. Kaučič, and R. W. Thompson, *Stud. Surf. Sci. Catal*. **125** (1999) 13–20.
30. I. Krznarić, T. Antonić, and B. Subotić, *Zeolites* **19** (1997) 29.
31. I. Krznarić, T. Antonić, and B. Subotić, *Microporous Mesoporous Mater.* **20** (1998) 161–175.
32. I. Krznarić, and B. Subotić, *Microporous Mesoporous Mater.* **28** (1999) 415–425.
33. E. Thilo, W. Wieker and H. Stade, *Z. Anorg. Allg. Chem.* **340** (1965) 261–276.
34. A. Katović, B. Subotić, I. Šmit, and LJ. A. Despotović, *Zeolites* **10** (1990) 634–641.
35. T. L. O'Connor, *J. Phys. Chem.* **65** (1961) 1–5.
36. B. D. Cullity, *Elements of X-ray Diffraction*, Addison-Wesley, Reading, MA, 1978.
37. G. B. Alexander, *J. Am. Chem. Soc.* **75** (1953) 5655–5657.
38. E. Wieker and B. Fahlke, *Stud. Surf. Sci. Catal.* **24** (1985) 161–181.
39. R. M. Barrer, *Hydrothermal Chemistry of Zeolites*, Academic Press, London, 1982, pp. 106–108.
40. G. Engelhardt, B. Fahlke, M. Mägi, and E. Lippmaa, *Zeolites* **5** (1985) 49–52.
41. A. V. McCormick, A. T. Bell, and C. J. Radke, *J. Phys. Chem.* **93** (1989) 1741–1744.
42. L. S. Dent Glasser and E. E. Lachowski, *J. Chem. Soc., Dalton Trans.* (1980) 399–402.
43. L. S. Dent Glasser, *Chem. Br.* (1982) 33–39.
44. A. T. Bell, A. V. McCormick, W. M. Hendricks, and C. J. Radke, *Chem. Express* **1** (1986) 687–690.
45. S. P. Zhdanov, *Adv. Chem. Ser.* **101** (1971) 20–43.
46. G. Harvey and L. D. Dent Glasser, *ACS Symp. Ser.* **398** (1989) 49–65.
47. Y. Yan, S. R. Chaudhuri, and A. Sarkar, *Chem. Mater.* **8** (1996) 473–497.

48. L. Gora, K. Streletzky, R. W. Thompson, and G. D. J. Phillies, *Zeolites* **19** (1997) 98–106
49. S. Mintova, N. H. Olson, V. Valtchev, and T. Bein, *Science* **283** (1999) 958–960.
50. L. A. Bursill and J. M. Thomas, in: R. Sersale, C. Collela, and R. Aielo (Eds.), *5th International Zeolite Conference: Recent Progress Report and Discussion*, Giannini, Naples, 1981, pp. 25–30.
51. B. Subotić and A. Graovac, *Stud. Surf. Sci. Catal.* **24** (1985) 199–206.
52. P. K. Dutta, D. C. Shieh, and M. J. Puri, *J. Phys. Chem.* **91** (1987) 2332–2236.
53. O. Okamura, Y. Tsuruta, and T. Satoh, *Gypsum Lime* **206** (1987) 23–28.
54. R. Aiello, F. Crea, A. Nastro, B. Subotić, and F. Testa, *Zeolites* **11** (1991) 767–775.
55. C. D. Chang and A. T. Bell, *Catal. Lett.* **8** (1991) 305–316.
56. K.-H. Yi and S.-K. Ihm, *Microporous Mater.* **1** (1993) 115–122.
57. M. D. Richards and C. G. Pope, *J. Chem. Soc., Faraday Trans.* **92** (1996) 317–323.
58. J. Bronić and B. Subotić, *Microporous Mater.* **4** (1995) 239–242..
59. T. Brar, P. France, and P. G. Smirniotis, *Ind. Eng. Chem. Res.* **40** (2001) 1133–1139.
60. I. Krznarić, T. Antonić, B. Subotić, and V. Babić-Ivančić, *Thermochim. Acta* **317** (1998) 73–84.
61. T. Antonić, B. Subotić, and N. Stubičar, *Zeolites* **18** (1997) 291–300.
62. B. Subotić, T. Antonić, I. Šmit, R. Aiello F. Crea, A. Nastro, and F. Testa, in: M. L. Occelli and H. Kessler (Eds), *Synthesis of Porous Materials: Zeolites, Clays and Microstructures*, Marcel Dekker Inc., New York-Basel-Hong Kong, 1996, pp. 35–
63. S. Bosnar and B. Subotić, *Microporous Mesoporous Mater*, **28** (1999) 483–493.
64. S. Bosnar, Ph.D. Thesis, University of Zagreb, 2000.
65. A. Katović, B. Subotić, I. Šmit, LJ. A. Despotović, and M. Ćurić, in: M. L. Occelli and H. E. Robson (Eds.), *Zeolite Synthesis*, *ACS Symp. Ser. No. 398*, Am. Chem. Soc., 1989, pp. 124–139.
66. M. Tatič and B. Držaj, *Stud. Surf. Sci. Catal.* **24** (1985) 129–136.
67. E. I. Basaldella and J. C. Tara, *Zeolites* **15** (1995) 243–246.
68. Y. Traa and R. W. Thompson, *J. Mater. Chem.* **12** (2002) 496–499.
69. B. Subotić, I. Šmit, O. Hadžija, and L. Sekovanić, *Zeolites* **2** (1982) 135–142.
70. S. Ma, L. Li, R. Xu, and Z. Yie, *Stud. Surf. Sci. Catal.* **24** (1985) 191–198.

SAŽETAK

Utjecaj izvora silikata na kemijski sastav hidrogelova i rezultate njihove hidrotermalne obradbe

Ivan Krznarić, Tatjana Antonić, Josip Bronić, Boris Subotić i Robert W. Thompson

Od mnogobrojnih čimbenika koji utječu na tijek hidrotermalne sinteze molekulskih sita (zeolita), utjecaj različitih izvora silikata najmanje je poznat. Prethodna su istraživanja pokazala da su neki izvori silikata »aktivni« ili »neaktivni«, a postoje indikacije da aluminij kao nečistoća pridonosi aktivnosti silikata u poboljšanju procesa sinteze zeolita. Iako je aktivnost izvora silikata u procesu kristalizacije zeolita nedvojbeno utvrđena, definitivno nije poznata jasna veza između aktivnosti i specifičnih nečistoća. U ovom je istraživanju razmatran utjecaj četiri različita izvora silikata na raspodjelu Na, Al i Si između tekuće faze i amorfnog gela. Pokazano je da je raspodjela Na, Al i Si neovisna o izvoru silikata, ali se mijenja sa sastavom reakcijske smjese. Stupanj polikondenzacije silikatnih aniona, mjeren molibdatnom metodom, također ne ovisi o izboru izvora silikata. Uočene razlike čestičnih i strukturnih svojstava produkata kristaliziranih iz hidrogelova pripravljenih korištenjem četiri različita izvora silikata razmatrane su s obzirom na kritične procese kristalizacije zeolita (otapanje gela, nukleacija i rast kristala).